Available online at www.sciencedirect.com
ScienceDirect
Bioorganic & Medicinal Chemistry Letters
Bioorganic & Medicinal Chemistry Letters 17 (2007) 4562–4567

Benzo[*b*]thiophene-based histone deacetylase inhibitors

David J. Witter,[a,*] Sandro Belvedere,[b] Liqiang Chen,[c] J. Paul Secrist,[a] Ralph T. Mosley[d] and Thomas A. Miller[a]

[a]*Merck Research Laboratories, Departments of Drug Design & Optimization and Cancer & Biology Therapeutics, 33 Avenue Louis Pasteur, Boston, MA 02115, USA*
[b]*ARMGO Pharma, Inc., 3960 Broadway 3rd Floor, New York, NY 10032, USA*
[c]*Center for Drug Design, University of Minnesota, 516 Delaware St. SE, Minneapolis, MN 55455, USA*
[d]*Department of Medicinal Chemistry, Merck Research Laboratories, 126 Lincoln Avenue, Rahway, NJ 07065, USA*

Received 5 April 2007; revised 29 May 2007; accepted 30 May 2007
Available online 6 June 2007

Abstract—Benzo[*b*]thienyl hydroxamic acids, a novel class of histone deacetylase (HDAC) inhibitors, were identified via a targeted screen of small molecule hydroxamic acids. Various substitutions were explored in the C5- and C6-positions of the benzo[*b*]thiophene core to characterize SAR and develop optimal inhibitors. It was determined that substitution at the C6-position of the benzo[*b*]thiophene core with a three-atom spacer yielded optimal HDAC1 inhibition and anti-proliferative activity in murine erythroleukemia (SC-9) cells.

Class I/II histone deacetylase (HDAC) enzymes are an emerging therapeutic target for the treatment of cancer and other diseases.[1] These enzymes, as part of multiprotein complexes, catalyze the removal of acetyl groups from lysine residues on proteins, including histones, affecting gene expression, differentiation, growth arrest, and/or apoptosis in transformed cell cultures.[2] HDAC inhibitors have been shown to bind directly to the HDAC active site and thereby block substrate access and cause the accumulation of acetylated histones in vitro.[2] In vivo xenograft studies[2] have further demonstrated many of these agents to be effective in the inhibition of tumor growth, and most recently, Zolinza™ (SAHA, vorinostat)[3] was approved for the treatment of the cutaneous manifestations of cutaneous T-cell lymphoma. A wide range of structures have been shown to inhibit the activity of Class I/II HDAC enzymes and, with few exceptions, these can be broadly characterized by a common pharmacophore comprised of a metal binding domain, a linker domain, and a surface recognition domain (Fig. 1).[4]

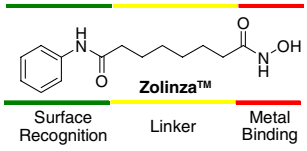

Figure 1. Pharmacophoric summary of HDAC inhibitors.

As part of an ongoing effort to identify novel HDAC inhibitors, a panel of small molecules containing hydroxamic acid metal binding moieties was screened for inhibitory activity against a crudely purified HDAC1 enzyme preparation.[5] These hydroxamic acids contained both the metal binding and linker domains but lacked the surface recognition domain, thereby allowing maximal conformational freedom and highest potential for obtaining the most favorable interaction between the active site zinc and the hydroxamic acid. Once active hydroxamic acid-based scaffolds were identified, the strategy was to perform subsequent modifications to the surface recognition domain to optimize potency and pharmacokinetic properties. During the initial scaffold 'scan' it was determined that there was a 30-fold increase in HDAC inhibitory activity progressing from aceto- to benzoyl hydroxamic acid, with IC_{50} values of 625 and 20 μM, respectively (Fig. 2). Further increases in HDAC inhibitory potency were realized by replacement of the aromatic phenyl moiety with a thiophene

Keywords: HDAC; Histone deacetylase inhibitor; HDAC inhibitor; Anticancer drug; SAHA; Hydroxamic acids; Benzo[*b*]thiophene.
* Corresponding author. Tel.: +1 617 992 2067; e-mail: David_Witter@merck.com

0960-894X/$ - see front matter © 2007 Elsevier Ltd. All rights reserved.
doi:10.1016/j.bmcl.2007.05.091

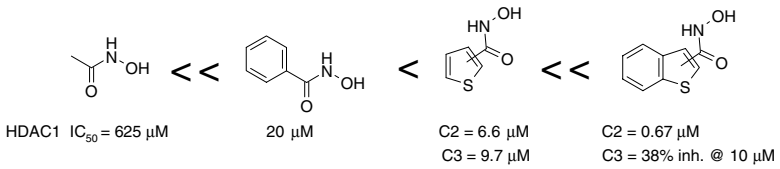

Figure 2. Representative SAR from initial scaffold 'scan'.

or benzo[*b*]thiophene (Fig. 2). The position of the hydroxamic acid on the core scaffold was determined to be important for both heterocycles, with the 2-substitution being optimal in both cases. The C3-hydroxamic acid on the benzo[*b*]thiophene exhibited 38% inhibition at 10 μM compared to 670 nM for the 2-substituted analog. Based on the 30-fold improvement in IC_{50} with the benzo[*b*]thiophene analogs relative to the phenyl, an exploration into benzo[*b*]thiophene substitutions was initiated.[6]

The benzo[*b*]thiophene moiety represents an important core structure found in biologically active small molecules ranging from protease inhibitors[7] to modulators of GPCRs[8] exemplified by marketed drugs such as Zileuton™,[9] and Raloxifene™.[8c] Like many other heterocyclic aromatic structures, the benzo[*b*]thiophene core provides numerous avenues for further chemical modifications and there has been an increasing interest in the development of methodologies for its construction.[10] In the present communication, we describe part of these SAR studies modifying the C5- and C6-positions of the benzo[*b*]thiophene core, focusing on the identification of the optimal substitution pattern.

Commercially available benzaldehyde **1** underwent cyclization with methyl thioglycolate to give benzo[*b*]thiophene di-methylester **3**, which was successfully converted into the desired monoacid **5** in excellent yield under standard saponification conditions (Scheme 1). Even though more than stoichiometric amount of sodium hydroxide (1.3 equiv) was used, this method yielded only one monoacid, together with small amounts of remaining di-methylester **3** and the corresponding diacid. Unfortunately, when di-methylester 4 was subjected to similar conditions, two inseparable monoacids were observed (ca. 2:1). In order to obtain a differentially substituted benzothiophene 2,5-dicarboxylate, the use of a *tert*-butyl protecting group was employed via a condensation reaction between benzaldehyde **2** and *tert*-butyl thioglycolate, which was prepared in situ from *tert*-butyl chloroacetate. Even though diester **6** was formed in low yield, subsequent deprotection of *tert*-butyl ester quantitatively afforded desired monoacid **7**. With both mono-acids in hand, trityl-protected hydroxylamine was used to afford the protected hydroxamic acids, which were converted to the free acids. Various amides were then constructed via standard amide coupling and the hydroxamic acids were deprotected (Scheme 1).

Acylated amino-benzo[*b*]thiothiophene analogs, **13a**–**g**, were prepared from commercially available nitro-benzothiophenes via hydrogenolysis to the amines, subsequent acylation, and conversion of the remaining ester to the hydroxamic acids (Scheme 2).[11] In order to generate the homologated aminomethyl analogs (Scheme 4), the formyl-benzo[*b*]thiophenes were synthesized as shown in Schemes 2 and 3. The 5-formyl benzo[*b*]thiophene **16** was made from diazonium salt formation followed by displacement with iodide which furnished the iodo derivative **14** in a modest yield (Scheme 2). Formation of a carbanion was accomplished by the action of isopropylmagnesium bromide at −40 °C in the presence of the ethyl ester. Subsequent formylation was initially attempted with DMF, but with little success. When the more reactive Meyer's reagent was used, the formy-

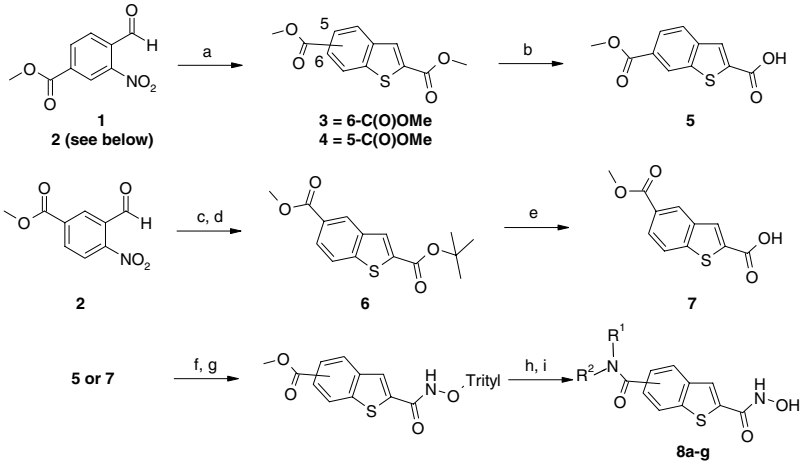

Scheme 1. Reagents: (a) $MeOC(O)CH_2SH$, K_2CO_3, DMF; (b) NaOH, THF/MeOH; (c) *t*-$BuOC(O)CH_2Cl$, NaSH, DCM; (d) K_2CO_3, DMF; (e) TFA, DCM; (f) Trityl-ONH_2, EDC, HOBt, DCM; (g) NaOH, THF/MeOH; (h) HNR^1R^2, EDC, HOBt, DCM; (i) TFA, DCM.

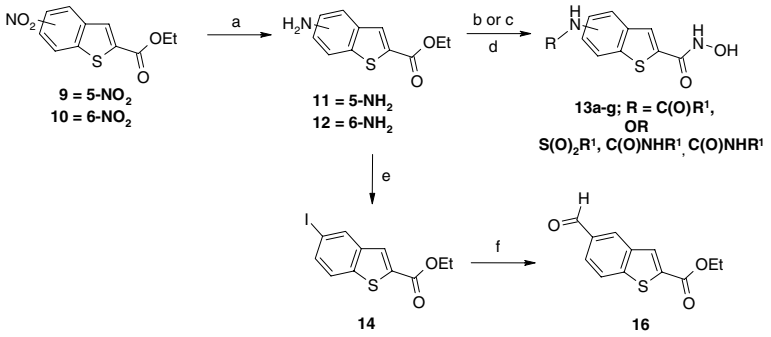

Scheme 2. Reagents and conditions: (a) H_2, Pd/C, EtOH; (b) $R^1C(O)Cl$ or $R^1S(O)_2Cl$, Et_3N, DCM; (c) R^1-NCO, DCM; (d) NH_2OH (aq), MeOH; (e) $NaNO_2$, H_2O, HCl, then NaI; (f) *i*-PrMgBr, THF, −40 °C, then Meyer's reagent.

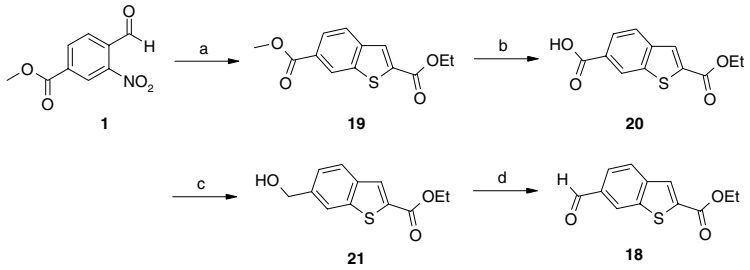

Scheme 3. Reagents and condition: (a) $EtOC(O)CH_2SH$, K_2CO_3, DMF; (b) LiI, pyr, reflux; (c) BH_3, THF; (d) MnO_2, DCM.

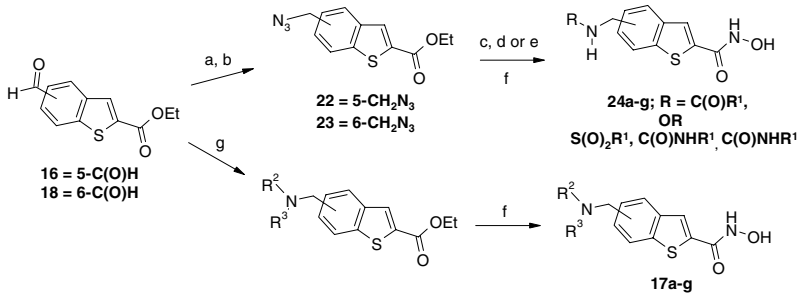

Scheme 4. Reagents: (a) $NaBH_4$, THF/EtOH; (b) $(PhO)_2P(O)N_3$, DBU; (c) H_2, Pd/C, MeOH; (d) $R^1C(O)Cl$ or $R^1S(O)_2Cl$, Et_3N, DCM; (e) R^1-NCO, DCM; (f) NH_2OH (aq), MeOH; (g) $NaBH(OAc)_3$, HNR^2R^3, DCE.

lation provided 5-formyl benzo[*b*]thiophene **16** in a 48% yield after crystallization. It should be noted that preparation of compound **16** from **9** using this sequence required no column chromatography.

For the preparation of 6-formyl benzo[*b*]thiophene **18**, a different approach was taken (Scheme 3). Condensation of benzaldehyde **1** with ethyl thioglycolate gave the benzo[*b*]thiophene **19**, containing both a methyl and an ethyl ester. Selective deprotection of methyl ester was accomplished using KI in refluxing pyridine generating monoacid **20** in 53% yield. Clean reduction of monoacid **20** with borane provided 6-hydroxymethyl **21**, which was subsequently oxidized to 6-formylbenzo[*b*]thiophene **18** in high yield. Both the 5- and 6-formyl benz[*b*]thiophenes, **16** and **18**, were used as intermediates.

Multiple analogs were generated from the common aldehyde intermediates (Scheme 4). The acylated aminomethyl analogs were generated from reduction of the aldehyde and subsequent conversion to the methyl azides, **22** and **23**. Hydrogenolysis of the azides generated the free amines, which were acylated and converted to the hydroxamic acids with aqueous hydroxylamine. The 2° and 3° amines were generated via reduction alkylation and conversion of the ester to hydroxamic acids as above.

All compounds were tested for the ability to inhibit HDAC1 activity and erythroleukemia cell proliferation. The initial series tested were the bis-oxo analogs represented in Table 1.[5] The data reveal that optimal surface recognition domain constituents are hydrophobic aromatic moieties residing in the benzo[*b*]thiophene C6-position. Moving from the methyl ester **8a** to the anilide **8c**, the HDAC1 potency is maintained, but there is an increase in cellular potency from 14 to 2.8 μM. Moreover, there appears to be an optimal chain length between the heterocycle and the phenyl moiety. A single methylene

Table 1. SAR of bis-oxo benzo[*b*]thiophene analogs

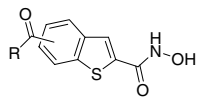

	R	Benzo[*b*]thiophene substitution	HDAC1 IC_{50} (nM)	SC9 IC_{50} (nM)
8a	OMe	6	630	13880
8c	PhNH	6	615	2775
8d	PhNH	5	600	6135
8e	$(Ph)CH_2NH$	6	55	1105
8f	$(Ph)CH_2NH$	5	75	1705
8g	$Ph(CH_2)_2NH$	6	60	2075
8h	$Ph(CH_2)_2NH$	5	155	5330
8i	$(Ph)_2CHNH$	6	285	2960

Values are means of three experiments.

spacer between these moieties results in an increase in cell potency as seen when comparing **8c**, **8e**, and **8g**. The maximal activity of the benzyl amide **8e** is reduced as the chain length increases to the phenethyl analog **8g**. Additional branching did not improve activity, as seen with biphenyl analog **8i**. In almost all cases the enzymatic and cellular inhibitory activities were superior for the 6-substituted benzothiophenes relative to the 5-position. The relatively poor cellular activity of the bis-oxo class of compounds prompted the search for alterative substitutions.

The next series of benzo[*b*]thiophene modifications investigated were aniline-based analogs of the benzo[*b*]thiophene core (Table 2). Acylations of the amino-benzo[*b*]thiophene yielded sulfonamides, ureas, carbamates, and amides. The sulfonamides, ureas, and carbamate analogs were shown to be active HDAC inhibitors (IC_{50} < 200 nM), but lacked the desired cellular activity (IC_{50} > 1 μM; data not shown). However, improvements in cellular activity were seen in the corresponding amide series. As seen with the bis-oxo series, hydrophobic aromatic moieties are preferred in the surface recognition domain and a similar SAR for linker length is observed. As the aromatic group is extended from the benzoylyl **13a**, phenylacetyl **13b**, to dihydrocinnamoyl **13d**, HDAC1 and cellular activities are maximal with an optimal three-atom linker **13b**. The enzymatic and cellular IC_{50}s for the phenylacetyl amide, **13b**, are sub-micromolar, 11 and 220 nM, respectively. Substitution of the pendent phenyl group had little effect on either activities as seen with **13e** and **13f**. Branching in the alpha-position of the phenylacetyl group revealed a mild dependence on stereochemistry as seen with the two enantiomers, **13h** and **13i**, where the *S*-enantiomer is threefold more active than its *R*-counterpart. Similar modifications were made in the 5-position, however 6-substitution offers superior HDAC1 and cellular activities (**13b** vs **13c**). The sub-micromolar SC9 activity seen with **13b** prompted analysis of the aniline-homologated amino-methyl benzo[*b*]thiophenes (Table 3).

To further investigate the enzymatic and cellular inhibitory activity of nitrogen-linked HDAC inhibitors, the homologated amino-methyl benzo[*b*]thiophenes were

Table 2. SAR of amide substituted benzo[*b*]thiophenes

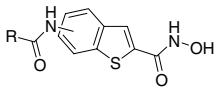

	R	Benzo[*b*]-thiophene substitution	HDAC1 IC_{50} (nM)	SC9 IC_{50} (nM)
13a	Ph	6	205	2900
13b	Bn	6	10	220
13c	Bn	5	30	1165
13d	Dihydro-cinnamoyl	6	55	5575
13e	(4-F)Ph–CH_2	6	20	230
13f	(4-OMe)Ph–CH_2	6	20	205
13g	(Ph)(Et)CH	6	40	225
13h	(Ph)((*S*)-Et)CH	6	20	140
13i	(Ph)((*R*)-Et)CH	6	60	530

Values are means of three experiments.

investigated. The initial analogs tested, the aminomethyl amines, displayed a similar trend as the amide series, with a three-atom linker being the optimal length (Table 3). Within the 6-substituted amines, optimal cellular activity (IC_{50} = 160 nM) is observed with the benzyl amine **17c**, relative to the corresponding aniline **17a** and phenethyl amine **17e**. The activity trend is similar for the 5-substituted amines, however, they are ~3-fold less potent than the corresponding 6-substituted analogs (**13b** vs **13c**).

Acylated aminomethyl analogs (Table 3), such as sulfonamides, carbamates, and ureas, exhibited HDAC enzymatic inhibition, but lacked potent cellular activity (data not shown; >1 μM). However, amide analogs possess both HDAC enzymatic and cellular activity. The benzoylamide **24a**, for example, possesses similar cellular activity compared to **17c** (190 vs 160 nM), suggesting the linker length between the hydrophobic aromatic group is an important driver of potency and not necessarily the functionality contained in the linker. As seen in the bis-oxo, amides, and amino-methyl analogs, there is a preference for C6-benzo[*b*]thiophene substitution with a linker length of three atoms between the terminal aromatic group and the benzothiophene core.

Table 3. SAR of homologated analogs

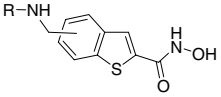

	R	Benzo[*b*]thiophene substitution	HDAC1 IC_{50} (nM)	SC9 IC_{50} (nM)
17a	Ph	6	45	1780
17b	Ph	5	175	4870
17c	$PhCH_2$	6	50	160
17d	$PhCH_2$	5	145	475
17e	$Ph(CH_2)_2$	6	128	455
17e	$Ph(CH_2)_2$	5	200	945
24a	PhC(O)	6	10	190
24b	$PhCH_2C(O)$	6	70	1220

Values are means of three experiments.

In order to better understand the increased HDAC1 activity of the benzo[*b*]thiophenes, compounds **13a–c** were docked into a homology model of hHDAC1 the construction of which is described elsewhere.[12] A set of 150 conformers of **13a–c** were generated[13a] and energy minimized using MMFF94 with a distance-dependent dielectric of $2r$.[13b] Due to the rigidity afforded by the amide linker in conjunction with the planar nature of the 2-hydroxyamyl benzo[*b*]thiophene, these effectively reduced to eight conformers which were docked into the homology model by superposition of the hydroxymate moiety onto that of trichostatin A (TSA) as observed in the hHDAC8 crystal structure (PDB entry 1T64).[14] This was followed by energy minimization as above within context of the hHDAC1 homology model wherein residues falling within 10 Å of each conformer were held rigid while the sidechains of residues within 5 Å were energy-minimized in conjunction with the inhibitor. Figure 3 contains surface representations of the modeled HDAC1 enzyme and one of the lowest energy conformers for each of the three HDAC inhibitors, **13a–c**, as well as the crystallographic structure of TSA as complexed with hHDAC8. The dimethylamino-phenyl and adjacent carbonyl of TSA form a planar structure that makes contacts with residues at the rim and adjacent shallow groove. The rigidity and regiochemistry of the pendant amides of the benzo[*b*]thiophenes appeared to preclude this same type of interaction with the enzyme during the modeling studies. During the energy minimization process, the aromatic ring of Phe205 proximate to the methyl group in TSA rotates ~110° toward the solvent-exposed surface away from a position orthogonal to the S of the docked benzo[*b*]thiophene ring. Thus, it appears to stack with the aromatic linker rather than clash with it in a face to edge fashion. This also results in a larger opening for the linker. It is interesting to note that this rotation occurred during minimization of the conformer which made the most stabilizing interactions with the protein with the least amount of internal strain. This conformer is one of the eight considered for **13b**, the most potent of the three inhibitors studied in this fashion, and is depicted in magenta in Figure 3. The main difference among the benzo[*b*]thiophene inhibitors arises from the pendant aromatic moiety. In **13b**, the phenyl group can achieve close contact to the Glu98 backbone maximizing van der Waals interactions. The orientation of the pendant phenyl moiety of **13c** is toward the surface groove occupied by TSA's dimethylamino-phenyl group, but is packed less snugly and makes fewer contacts. For the least active inhibitor, **13a**, which is the truncated analog, the phenyl group is unable to utilize either of the above surface interactions.

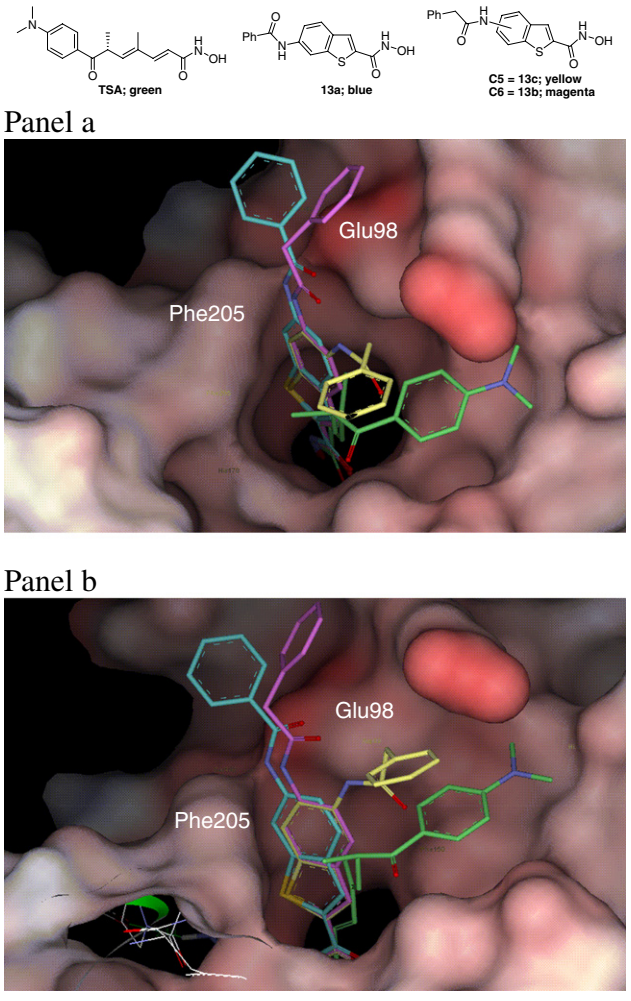

Figure 3. Panels a and b contain surface representations of a homology model of HDAC1 based on HDLP with docked HDAC inhibitors, TSA and **13a–c**. Each panel a and b represent a different spatial orientation of the HDAC1 surface to illustrate the binding differences among the four inhibitors. TSA is labeled in green, **13a** is in blue, **13b** is in magenta, and **13c** is in yellow. Preferred orientations of **13a–c** illustrate the optimal fit of **13b**.

In conclusion, we have identified a series of novel benzo[*b*]thiophene HDAC inhibitors that are characterized by high potency in HDAC and cellular proliferation assays. C5- and C6-substituted benzothiophenes were synthesized and the most active compounds were phenylacetyl amide, **13b**, benzylamine, **17c**, and benzoylamide, **24a**, which are C6-substituted. Moreover, all three structural series described herein were found to exhibit the same SAR with regard to the distance between the terminal aromatic moiety and the benzothiophene core. A three-atom linker proved to be optimal for HDAC1 activity and homology models revealed a favorable interaction for the C6-substitution pattern and linker length. Further studies of these agents and related analogs will be reported in due course.

References and notes

1. (a) Huang, L. *J. Cell. Physiol.* **2006**, *209*, 611; (b) Liu, T.; Kuljaca, S.; Tee, A.; Marshall, G. M. *Cancer Treat. Rev.* **2006**, *32*, 157; (c) Sadri-Vakili, G.; Cha, J.-H. J. *Curr. Alzh. Res.* **2006**, *3*, 403.
2. (a) Rodriquez, M.; Aquino, M.; Bruno, I.; De Martino, G.; Taddei, M.; Gomez-Paloma, L. *Curr. Med. Chem.* **2006**, *13*, 1119; (b) Dokmanovic, M.; Marks, P. A. *J. Cell. Biochem.* **2005**, *96*, 293.
3. Grant, S.; Easley, C.; Kirkpatrick, P. *Nat. Rev. Drug Discov.* **2007**, *6*, 21.
4. Miller, T. A.; Witter, D. J.; Belvedere, S. *J. Med. Chem.* **2003**, *46*, 5097.

5. HDAC activity (enzymatic) was evaluated with epitope-tagged human HDAC1 complex immuno-purified from stably expressing mammalian cells and substrate from Biomol Research Laboratories, Inc., Plymouth Meeting, PA. Cell-based HDAC activity was studied in a MTS assay using murine erythroleukemia cells (SC-9) incubated with vehicle or increasing concentrations of compound for 48 h. For full details, see: Miller, T. A.; Witter, D. J.; Belvedere, S. Preparation of thiophene and benzothiophene hydroxamic acid derivatives as histone deacetylase inhibitors. WO2005034880, 2005.
6. Structure–activity relationships of additional scaffolds will be highlighted in due course.
7. (a) Liang, A. M.; Light, D. R.; Kochanny, M.; Rumennik, G.; Trinh, L.; Lentz, D.; Post, P.; Morser, J.; Snider, M. *Biochem. Pharmacol.* **2003**, *65*, 1407; (b) Dellaria, J. F. US Patent 6,207,701, 2001; (c) Johnson, M. G.; Bronson, D. D.; Gillespie, J. E.; Gifford-Moore, D. S.; Kalter, K.; Lynch, M. P.; McCowan, J. R.; Redick, C. C.; Sall, D. J.; Smith, G. F.; Foglesong, R. J. *Tetrahedron* **1999**, *55*, 11641; (d) Yamashita, D. S.; Dong, X.; Oh, H.-J.; Brook, C. S.; Tomaszek, T. A.; Szewczuk, L.; Tew, D. G.; Veber, D. F. *J. Comb. Chem.* **1999**, *1*, 207.
8. (a) Halfpenny, P. R.; Horwell, D. C.; Hughes, J.; Hunter, J. C.; Rees, D. C. *J. Med. Chem.* **1990**, *33*, 286; (b) Moloney, G. P.; Garavelas, A.; Martin, G. R.; Maxwell, M.; Glen, R. C. *Eur. J. Med. Chem.* **2004**, *39*, 305; (c) Bradley, D. A.; Godfrey, A. G.; Schmid, C. R. *Tetrahedron Lett.* **1999**, *40*, 5155.
9. Carter, G. W.; Young, P. R.; Albert, D. H.; Bouska, J.; Dyer, R.; Bell, R. L.; Summers, J. B.; Brooks, D. W. *J. Pharmacol. Exp. Ther.* **1991**, *256*, 929.
10. Horton, D. A.; Bourne, G. T.; Smythe, M. L. *Chem. Rev.* **2003**, *103*, 893.
11. General experimental for acylated 6-amino-benzothiophenes. To a solution of 6-amino-benzo[*b*]thiophene-2-carboxylic acid methyl ester (75 mg, 0.36 mmol) and NMM (51.7 μL, 0.47 mmol) in THF/CH_2Cl_2 (2/1 mL) was added acid chloride (0.434 mmol). After 24 h, the solvent was removed. To the resultant mixture were added DMA (2 mL) and NH_2OH (50% aq, 1 mL). The solution was stirred until the disappearance of starting material as indicated by LC/MS. After removal of solvent, MeOH/H_2O was added until a precipitate formed. The solid was filtered yielding the desired amide (**13b**; 65% yield). ^1H NMR (DMSO-d_6) δ 11.38 (br s, 1H), 10.42 (br s, 1H), 9.21 (br s, 1H), 8.38 (s, 1H), 7.90–7.75 (m, 2H), 7.50–7.15 (m, 6H), 3.65 (s, 2H). MS (EI): calcd (MH^+) 327.07, exp (MH^+) 327.28. Additional experimental details and spectral data can be found in Ref. 5.
12. Hamblett, C. L.; Methot, J. L.; Mampreian, D. M.; Sloman, D. L.; Stanton, M. G.; Kral, A. M.; Fleming, J.; Cruz, J. C.; Chenard, M.; Ozerova, N.; Hitz, A. M.; Wang, H.; Deshmukh, S. V.; Harsch, A.; Middleton, R. E.; Mosley, R. T.; Secrist, J. P.; Miller, T. *Bioorg. Med. Chem. Lett.*, to be submitted.
13. (a) Crippen, C. M.; Havel, T. F. *Distance Geometry and Molecular Conformation*; Wiley: NewYork, 1988; (b) Halgren, T. A. *J. Comp. Chem.* **1999**, *20*, 720.
14. Somoza, J. R.; Skene, R. J.; Katz, B. A.; Mol, C.; Ho, J. D.; Jennings, A. J.; Luong, C.; Arvai, A.; Buggy, J. J.; Chi, E.; Tang, J.; Sang, B.-C.; Verner, E.; Wynands, R.; Leahy, E. M.; Dougan, D. R.; Snell, G.; Navre, M.; Knuth, M. W.; Swanson, R. V.; McRee, DE.; Tari, L. W. *Structure* **2004**, *12*, 1325.